REPORT No. 802

NACA INVESTIGATION OF A JET-PROPULSION SYSTEM APPLICABLE TO FLIGHT

By Macon C. Ellis, Jr., and Clinton E. Brown

SUMMARY

Following a brief history of the NACA investigation of jet propulsion, a discussion is given of the general investigation and analyses leading to the construction of the jet-propulsion ground-test mock-up. The results of burning experiments and of test measurements designed to allow quantitative flight-performance predictions of the system are presented and correlated with calculations. These calculations are then used to determine the performance of the system on the ground and in the air at various speeds and altitudes under various burning conditions. The application of the system to an experimental airplane is described and some performance predictions for this airplane are made.

It was found that the main fire could be restricted to an intense, small, and short annular blue flame burning steadily and under control in the intended combustion space. With these readily obtainable combustion conditions, the combustion chamber, the nozzle walls, and the surrounding structure could be maintained at normal temperatures. The system investigated was found to be capable of burning one-half the intake air up to fuel rates of 3 pounds per second. Calculations were shown to agree well with experiment. It was concluded that the basic features of the jet-propulsion system investigated in the ground-test mock-up were sufficiently developed to be considered applicable to flight installation. Calculations indicated that an airplane utilizing this jet-propulsion system would have unusual capabilities in the high-speed range above the speeds of conventional aircraft and would, in addition, have moderately long cruising ranges if only the engine were used.

INTRODUCTION

HISTORICAL DEVELOPMENT

A general study to investigate the possibilities of jet-propulsion systems was begun by the air-flow-research staff at Langley Memorial Aeronautical Laboratory in February 1939. The purpose of the study was to reevaluate Buckingham's work (reference 1) for speeds higher than those he considered reasonable but now being approached by propeller-driven airplanes. Results of this and subsequent studies indicated that a unit utilizing an efficient gasoline engine to drive a blower and duct system of reasonable efficiency was the most desirable experimental approach to the development of a jet-propulsion airplane. The airplane utilizing this system would be capable of realizing truly high powers from a high-temperature jet for short periods of time and would, in addition, be capable of moderately long cruising flight if only the engine were used.

Certain problems appeared to be involved in the application of the proposed jet-propulsion system, in particular those problems associated with the control of combustion in the relatively high-speed air stream in the combustion chamber. A simple program of burning experiments was therefore undertaken. A blower driven by an airplane engine was to be employed in order that burning experiments could be made with approximately full-scale equipment and in order that the engine exhaust might be available, if it should be desirable to make use of the exhaust in connection with the burners. While the necessary large-scale equipment was being built, some burning experiments, which gave useful information about the best methods to be tried later with the large-scale apparatus, were conducted with small-scale equipment.

At about this time, in March 1941, the Special Committee on Jet Propulsion, with Dr. W. F. Durand as chairman, was established by the National Advisory Committee for Aeronautics to guide this and other projects. Dr. Durand, in particular, then took an active interest in the project and since has considerably influenced the course of the work. Through Dr. Durand's influence at this time, the scope and the purpose of the work became markedly altered. The test setup became more nearly a mock-up of a proposed airplane for ground testing rather than simply a burner test rig. A more powerful engine than the one originally used was obtained from the Bureau of Aeronautics, but most of the parts already built were retained. The scope of the investigation was extended to include a study of the blower and duct characteristics as well as the action of burning; it was agreed that cheap and simple sheet-iron construction would be employed when possible to save time. Even with this construction, it was hoped that something would also be learned about how much of the air could be burned without producing excessive temperatures in the walls and structural parts of an airplane.

At this time, owing to the changed and extended scope of the work, the whole project should probably have been reexamined and parts, including the blower, redesigned and rebuilt. The necessity of such changes did not become clearly evident, however, until preliminary tests had been made with the original engine-blower and duct arrangement.

After much lost time, the necessary changes were made and the preliminary tests completed during July 1942. Some of the results of the experimental investigations, together with the applications of the results to some possible military airplanes, were reported to the NACA Special Committee on Jet Propulsion on October 6, 1942. The results of continued experimental investigations and analyses from October 6, 1942, to the time experimental work was halted, April 15, 1943, are given in the present report.

PURPOSES OF INVESTIGATION

In considering the test methods adopted, the two principal purposes of the investigation should be remembered:

(1) The original purpose—to obtain data, mainly qualitative, on burning methods and associated effects and limitations.

(2) The purpose proposed by the NACA Special Committee on Jet Propulsion—to obtain by straightforward test methods data, mainly on blower and duct characteristics, in order to provide a basis for quantitative flight-performance estimates.

GENERAL INVESTIGATION OF JET PROPULSION

Buckingham (reference 1) concluded that moderately high compression ratios would be required to realize a reasonable thermodynamic-cycle efficiency in converting the heat input into kinetic energy in the propulsion jet and that compressor machinery would be required comparable in size and weight with the gasoline engine which the jet-propulsion system might otherwise replace. With the low propulsive efficiencies associated with the high-speed propulsion jets, particularly at the relatively low speeds contemplated, and with little or no attendant weight advantage to offset this disadvantage, Buckingham concluded that jet-propulsion systems for aircraft showed little promise.

In order to reexamine these conclusions, approximate calculations for jet-propulsion systems were made in the speed range near 500 miles per hour. Compression ratios were considered that varied from the ratio obtained with only the dynamic-pressure compression up to ratios of 8 or 10. These calculations showed, for comparable conditions, surprisingly little or no clearly evident variation in over-all thermopropulsive efficiency with compression ratio. With increasing compression ratios, the gain in the thermodynamic-cycle efficiency (in converting heat into kinetic energy in the propulsion jet) thus tended to be almost exactly compensated by a corresponding loss in the propulsive efficiency associated with propulsion by means of a progressively smaller and higher-speed jet. With little variation in over-all efficiency with compression ratio, there remained nothing to recommend the higher range of compression ratio considered by Buckingham with the attendant compressor and prime mover of increasing power, size, and weight. A somewhat more detailed compression-ratio study was made for a system utilizing a compressor prime mover of constant thermal efficiency. Results of this study as presented in appendix A tend to confirm the early conclusion that high compression ratios might not necessarily be desirable for a system of this type.

The possibility of eliminating the compressor was suggested; the system would thus revert to the Meredith cycle, now well known through its application to the utilization of some of the heat dissipated in airplane cooling systems. Such a system, in which only the dynamic pressure is used for compression, is unsatisfactory in the take-off and low-speed flight range but may be of some interest as an auxiliary system on other aircraft, such as the conventional airplane, having other means of propulsion in the take-off and low-speed range.

The choice of a suitable prime mover for the compressor was next considered. A gas-turbine unit at first appeared to offer possibilities because some of the otherwise wasted heat in the exhaust might be used in the propulsion cycle. The same is true, however, when the gas turbine is used in the conventional airplane or when the conventional engine is used in the jet-propulsion airplane. The conventional engine not only gives higher thermal efficiencies and therefore better duration and range when cruising on engine only but is already well developed and dependable and in no sense experimental. It therefore seemed unwise to hamper a project intended primarily to develop the possibilities of jet propulsion by unnecessarily including components, such as a gas-turbine prime mover, which themselves must be treated as experimental.

AN EXPERIMENTAL AIRPLANE TO STUDY JET PROPULSION

At this stage of the investigation it appeared desirable to consider the application of the jet-propulsion system to an experimental airplane that could be flown in order to obtain conclusive results. The power of the engine should, of course, depend primarily on the size of the airplane to which the jet-propulsion system is to be applied. For experimental purposes it is advisable, from considerations of time and effort to be expended, to keep the airplane small. On the other hand, the airplane must be flight-tested to obtain conclusive results and must therefore carry a pilot and instrumental equipment. The airplane should be of sufficient dimensions and power that these items will not exert a marked adverse effect on the size and performance of the complete airplane. The Pratt & Whitney R–1535 Twin Wasp, Jr., engine was chosen primarily because of its unusually small diameter, which permitted ample duct space around the engine in a reasonably small fuselage.

FUEL-RATE CONSIDERATIONS

Calculations show that jet-propulsion systems generally have low thermopropulsive efficiencies while burning fuel in the combustion chamber to provide a truly high-power propulsion jet, even in the higher speed range below the speed of sound. Thermal efficiency is of little importance, however, for high-speed flight in modern pursuit-type airplanes as shown by the fact that modern air-cooled engines, for the military-power condition, are commonly supplied with twice the quantity of gasoline necessary for combustion. For combat purposes, therefore, advantages gained from the use of a large power output for a short period from an engine of a given size and weight evidently far outweigh any considerations of thermal efficiency. Jet-propulsion systems have the advantage in similar situations of permitting higher outputs than conventional power plants of a given size and weight.

A really fair comparison between the fuel rates for a conventional engine-propeller-driven airplane and for a jet-propulsion airplane of the type proposed is not feasible. If the engine of a comparable conventional airplane were boosted without increasing its size until the airplane would fly, say, 570 miles per hour, a comparison could be made at this speed; but the conventional airplane would be hypothetical. The propeller efficiency would probably be very low but could not be stated quantitatively. The low propeller efficiency would lead to a high fuel rate even if the specific fuel consumption of the engine did not increase with such an extreme boost. The weight of the engine and propeller would also be difficult to estimate with the result that the required increase in size and weight of the airplane and its power requirements would remain problematical. The fuel rate of the conventional airplane might be expected to be at least as high as the fuel rate of the jet-propulsion airplane and would probably be much higher. The fuel rate of the jet-propulsion airplane, moreover, can be predicted and the airplane can be built through the application of straightforward engineering; the conventional airplane cannot. The high fuel rate of either airplane at this speed is evidently the price that must be paid and has always been required for transport at increased speeds, although the price may be reduced by a change of method, such as the evolution from ocean to air transport. Possibilities of supersonic speeds at very high altitudes are being considered.

SCOPE OF INVESTIGATION

The results of experiments with the final ground-test apparatus are presented and compared with calculations designed to predict the performance of the jet-propulsion system in flight. An experimental jet-propulsion airplane is described and calculated items of performance are presented.

ACKNOWLEDGMENT

Acknowledgment is gratefully expressed for the expert guidance and many original contributions of Mr. Eastman N. Jacobs, who initiated and supervised this work.

SYMBOLS

p absolute pressure, pounds per square foot
Δp_b total-pressure rise through blower including blower and entrance losses, pounds per square foot
Δp static-pressure rise in combustion chamber including entrance, blower, and duct losses, pounds per square foot
ρ mass density, slugs per cubic foot
N engine and blower speed, rpm
P engine power, horsepower
Q quantity rate of flow, cubic feet per second
m mass rate of flow, slugs per second
V velocity, feet per second
V_0 flight velocity, feet per second
ΔV relative jet velocity, feet per second $(V_4 - V_0)$
L/D lift-drag ratio
M momentum, pounds; also, with subscript 0, Mach number

T absolute temperature, °F absolute
A area, square feet
g acceleration due to gravity, feet per second per second
c_p heat-capacity coefficient, Btu per pound per °F
R gas constant, foot-pounds per slug per °F
R' gas constant, Btu per pound per °F
H heat equivalent of fuel, Btu per second
γ ratio of specific heat at constant pressure to specific heat at constant volume
F_R fuel burning rate, pounds per second
η_b blower-duct efficiency
η_p thermopropulsive efficiency
η_e engine thermal efficiency
C_R effective blower-duct compression ratio at station 2
C_V dynamic compression ratio
f ratio of energy input to burner to energy input to engine

Subscripts:
0 atmospheric conditions
i impact conditions
1 station immediately after blower
2 station 2 in combustion chamber
3 station 3 in combustion chamber
4 station 4 at end of nozzle exit
2,3 from station 2 to station 3, and so forth

DESCRIPTION OF GROUND-TEST EQUIPMENT

All the essential parts of the ground-test setup of the jet-propulsion system are shown in the section drawing in figure 1. Except for the nose air-intake section, which is made of wood, the outer shell and air ducts are constructed of black iron. The nose shape represents the shape actually contemplated for the airplane except that, for the ground tests, the entrance cone shown in figure 1 was added to prevent separation at the nose for the static-test conditions. A discussion of the use of this entrance cone appears later in the present report. The two faired sections in the entrance air duct ahead of the blower simulate a cockpit for the pilot and a housing for the nose wheel.

The blower is of the axial-flow type and consists of two main stages and one engine-cooling stage; aluminum alloy is used throughout. The blower rotor is driven directly from the engine crankshaft and the blower housing and stator stages are fastened to the engine crankcase; the blower and engine are thus an integral unit. The engine used is a Pratt & Whitney R-1535 Twin Wasp, Jr., rated at 825 horsepower at 2630 rpm if 100-octane fuel is used.

The primary burner, which supplies vaporizing heat and superheat to the main boiler, is located behind the engine section across the mouth of the main boiler and receives its gasoline vapor from seven Inconel exhaust-tube boilers, each of which utilizes the exhaust heat from two engine cylinders. Ignition for the primary burner is provided by two spark plugs located at the top and bottom of the burner.

The main boiler is made up of 24 separate Inconel tubes fed by a common manifold containing 24 calibrated metering orifices in the fuel outlets. In the first part of the boiler, the tubes are coiled spirally inside an Inconel sheet, which is a continuation of the engine-cooling-air duct. In the second
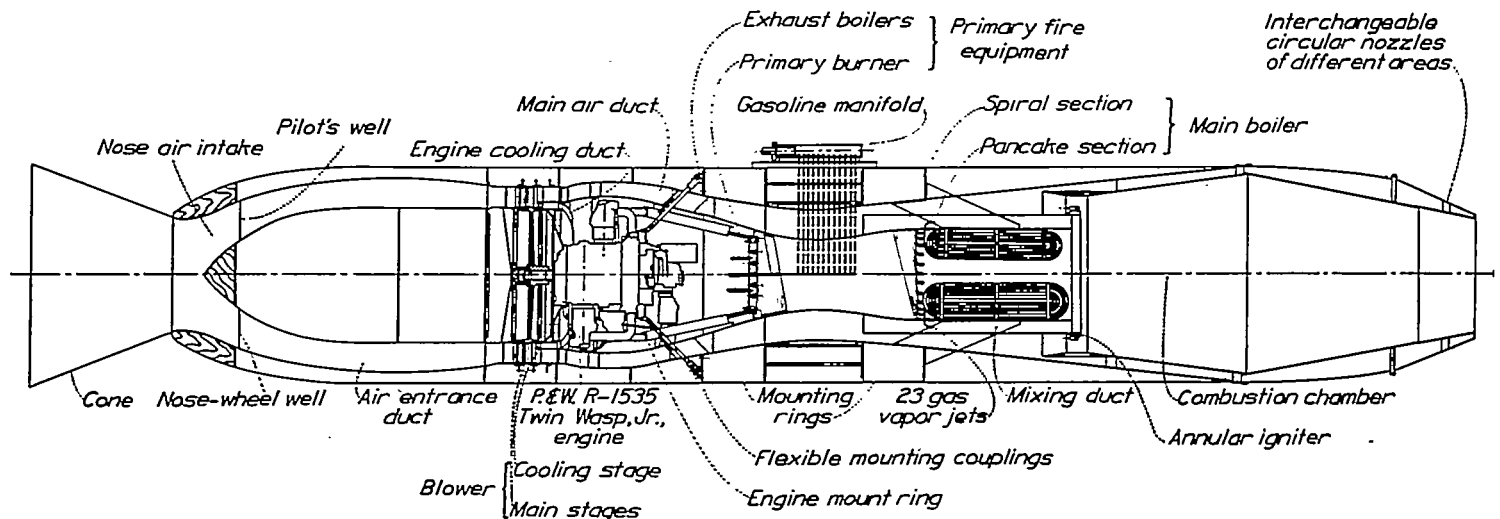
FIGURE 1.—Ground-test mock-up.

or superheating part of the boiler, each of the 24 tubes is wrapped into two flat coils, which are connected in series and mounted radially in the duct. The tube ends are led out through the Inconel shell to jets located in the mixing-duct entrance. The air-fuel mixture at the end of the mixing duct is ignited by a flame from a ring burner. This annular igniter is fed vapor from one of the 24 main boiler tubes and is initially ignited by two sparks 180° apart.

The black-iron combustion chamber was designed to provide a blanket of air on both the inside and the outside of the chamber wall and the exit nozzle. The several exit nozzles used for the ground tests were interchangeable and of various areas.

For the purpose of measuring the static thrust, the entire ground-test mock-up is mounted on three ball-bearing wheels, which roll on sections of steel track. The thrust is indicated by a sensitive dial gage that measures the deflection of a calibrated U-spring dynamometer.

TEST RESULTS AND DISCUSSION

COMBUSTION RESULTS

In accordance with the original purpose of the investigation, the test procedure consisted of a series of observations of burning under various conditions. Many such qualitative observations were accomplished with model burning experiments and led to the conclusion that a blue flame would be advantageous. These experiments also indicated the most promising methods, which were later used in the burning experiments with the full-scale apparatus.

It may be said that the results of the full-scale burning experiments generally exceeded expectations. The main fire was restricted to an intense, small, and short annular blue flame burning steadily and under control in the intended combustion space. In fact, in the last series of experiments, burning runs lasting 7 to 9 minutes were consistently made with hands-off operation. The results exceeded expectations in that satisfactory flames were obtained up to fuel rates corresponding to burning approximately one-half the air passing through the entire system. Under these conditions, the temperatures in parts of the jet must be very high and

even if complete mixing with all the cooling air—an impossible condition—were assumed, the mean temperature would be almost 2200° F. Even this fictitiously low temperature corresponds to bright yellow black-body radiation. In the presence of the burner flames and jet air at 2200° F and much higher temperatures, the black-iron liner forming the actual combustion chamber and nozzle wall, which was expected to require the use of stainless steel or other heat-resistant material, became only hot enough to blue the iron in a few spots. These spots were probably the result of only transient or locally defective conditions. Under these conditions, the outside shell became only slightly warm.

From the burning experiments, it was concluded that, with proper conditions, a blanket of cool air can be maintained between the hot gases and the walls. In the presence of suitable combustion, furthermore, adequate cooling air may readily be provided to carry away any radiant heat and to maintain the walls and structure at normal temperatures. It is believed that the foregoing conclusions, together with the information that has been gained about combustion, constitute the new and really significant results of the present investigation.

The operation of the burning system was satisfactory in all respects with the possible exception of one detail. During one of the burning experiments, it was noticed that the flow had stopped through one of the boiler tubes. An inspection of this and several other tubes indicated that the inner surfaces of the tubes were generally clean. A plug of carbon, which was removed by probing and blowing out the tube, had apparently collected, however, in the radial superheat unit at the end of the defective tube. Air was subsequently passed through all the boiler tubes while they were kept at red heat by means of the primary fire, with the object of burning out any carbon deposits in the rest of the tubes. During this process, hot spots were seen to develop on some of the tubes, which indicated that other carbon deposits were burned out by the process. It may be that some such simple carbon-removing process would be required as part of the service on these boiler-type burning systems.

BLOWER-DUCT CHARACTERISTICS

The experimental results to provide a basis for performance predictions, in accordance with the second purpose of the investigation, consist mainly of measurements of engine-blower and duct characteristics in the cold condition. These experimental data then form the basis for straightforward engineering calculations for operation of the system in the static and flight conditions at various speeds and with various amounts of gasoline burned to provide various jet temperatures.

The required experimentally determined blower-duct-system data are presented in figure 2. The data were taken directly from measurements and are presented in the slightly altered form indicated in figure 2 to make them approximately independent of power, engine speed, and density ρ. The blower pressure coefficient $\Delta p_b/\rho N^2$ is treated throughout as the independent variable. During experiments or during flight, the value of $\Delta p_b/\rho N^2$ would be determined by a suitable adjustment of the tail opening to give the desired blower conditions.
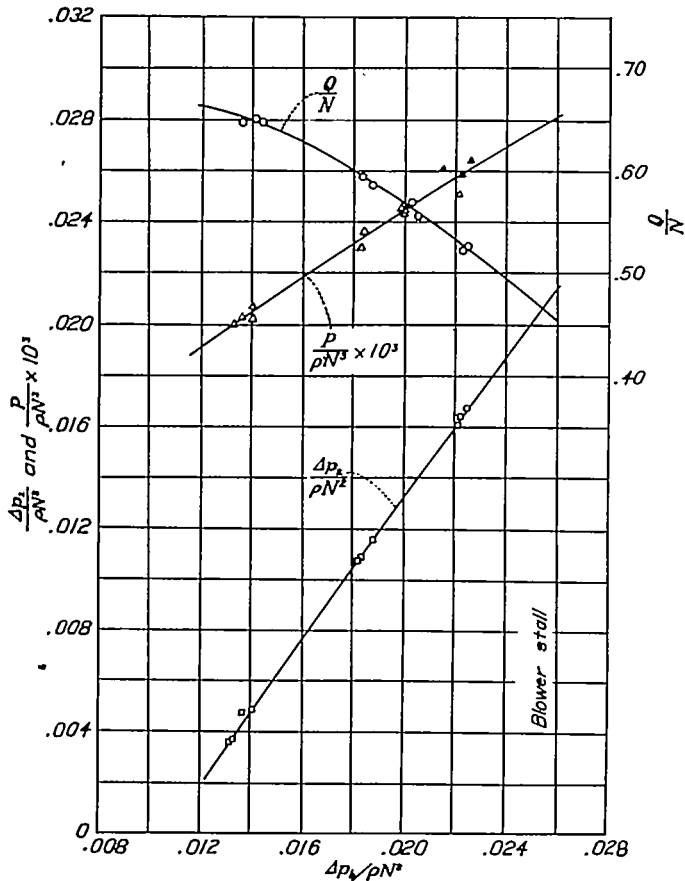

FIGURE 2.—Performance characteristics as determined from static tests of blower-duct system.

The curve representing the power absorbed by the blower was obtained from several tests at engine speeds of 1600, 1800, and 2000 rpm. The power was obtained from the calibration chart furnished by the manufacturer for the engine in terms of engine speed, manifold pressure, and carburetor-air temperature. The error in power may thus be larger than in most other measurements but a power lower than that indicated during the tests, which is most likely,

represents a conservative error because the indicated power tends to make the blower-duct system appear less efficient.

The quantity curve Q/N was determined from pressures indicated by a calibrated static orifice located inside the fuselage-nose air entrance at the minimum-area section. The orifice was calibrated by making a series of pressure surveys across the nose at the orifice station and over the exit nozzle.

The useful part of the output of the blower-duct system is measured by Q and Δp_2, the static pressure in the combustion chamber. This important output term is given in figure 2 as $\Delta p_2/\rho N^2$ and includes all of the entrance, blower, and duct losses at least back to the combustion chamber with one exception that must now be briefly considered.

Preliminary flow observations showed that the flow at the fuselage-nose air entrance would lead to rather large losses through a tendency under static-test conditions to develop separation inside the duct entrance lip. It was expected that this loss would be greatly reduced in any practical case in which forward speed would be available to aid the entrance flow. This expectation was verified by means of a small-scale-model test of the apparatus in the NACA two-dimensional low-turbulence pressure tunnel. The loss was shown to become negligible at take-off speeds and higher and to be greatly reduced even in the static condition if the airplane were facing into an ordinary gentle breeze. For the later parts of the take-off run, when the thrust and distance covered become of greatest importance, and particularly for the higher pressure coefficients and lower values of quantity flow that would be employed, this loss becomes unimportant. On the other hand, static measurements with this entrance loss included would have been spurious and subject to marked variations with slight changes in wind conditions. The wind-tunnel tests showed that the difficulty could be overcome by the addition of a cone to the fuselage-nose air entrance. A similar cone, as shown in figure 1, was therefore added to the ground-test mock-up but of course would be omitted as entirely unnecessary on any practical application to an airplane.

STATIC THRUST

Cold.—The curves of sea-level blower load and engine power are shown in figure 3. The intersections indicate the speed and power input to the blower that correspond to static-thrust conditions at sea level. The particular engine used in the ground-test mock-up is rated at 825 horsepower at 2630 rpm; this power is delivered at approximately 38 inches of mercury manifold pressure at sea level. In order to estimate the performance of an airplane utilizing the jet-propulsion system investigated, the engine output at 46 inches of mercury manifold pressure is shown in figure 3. This higher output is an estimate made from statements of representatives of the engine manufacturer that the engine used could be "modernized" to deliver approximately 1200 horsepower at 2800 rpm. The blower in the ground-test mock-up, however, was not designed to exceed the original rated speed of the engine; 2630 rpm is therefore shown in figure 3 and is taken throughout the present report as the limiting blower speed.
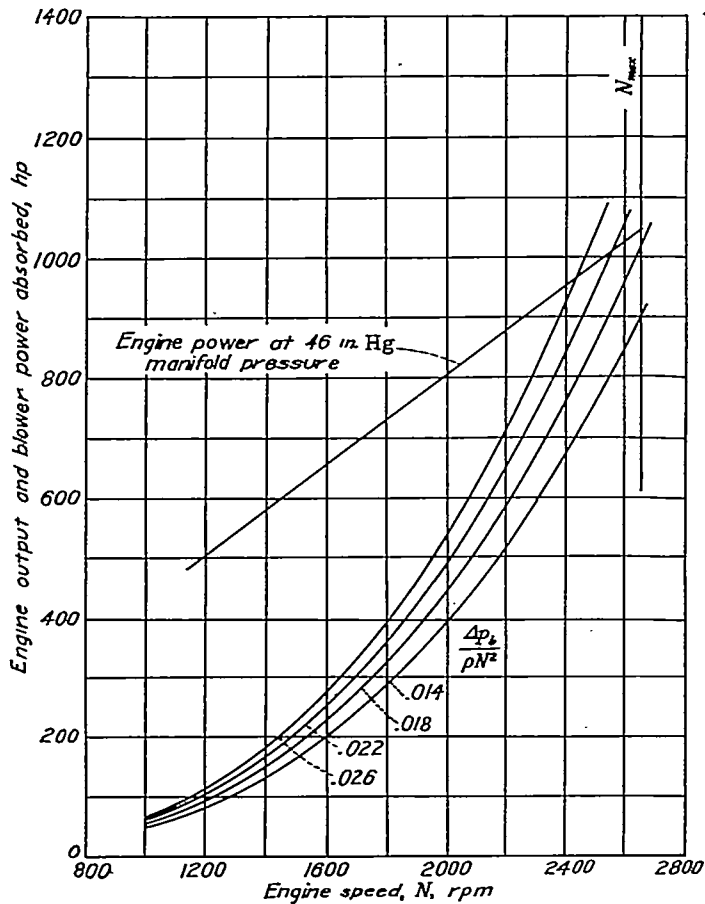
FIGURE 3.—Engine output and blower power absorbed for jet-propulsion system at sea-level conditions. $\rho=0.002378$.
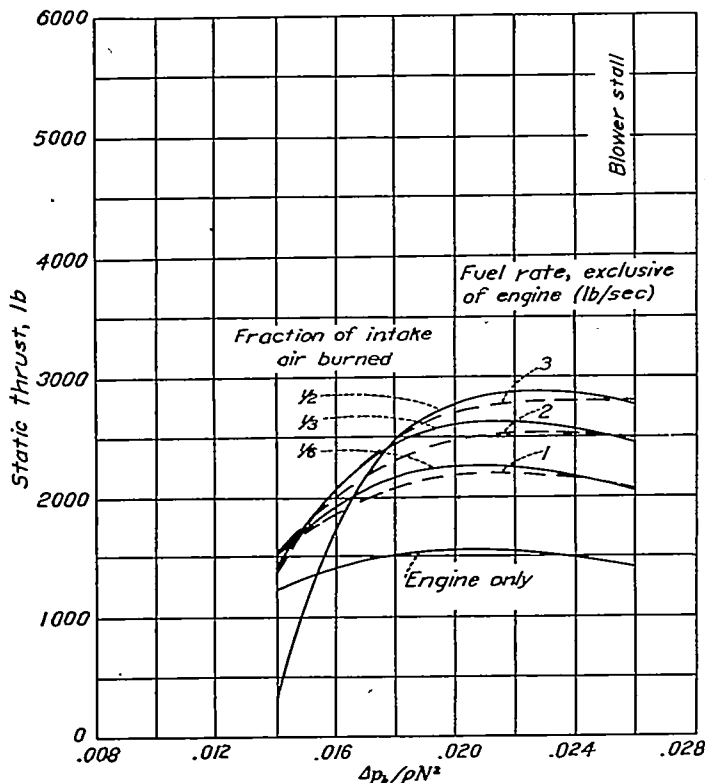

FIGURE 4.—Variation of static thrust with blower pressure coefficient for jet-propulsion system for various burning conditions and for engine only.
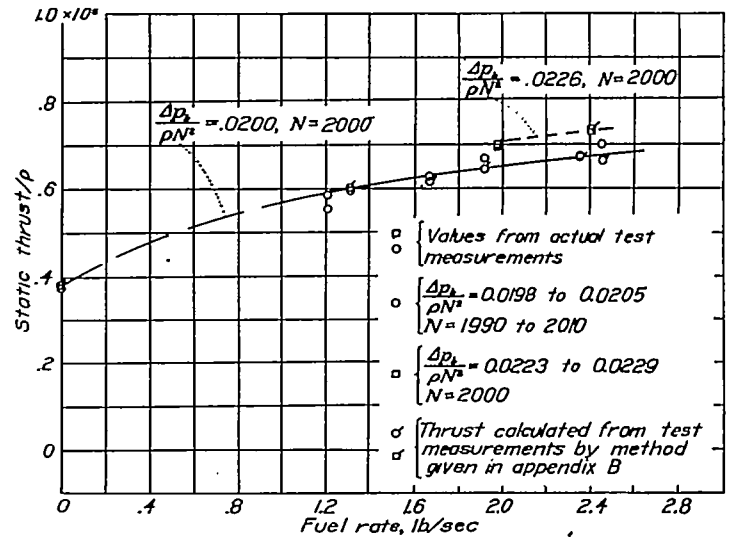

FIGURE 5.—Comparison of variation of measured and calculated static thrust with fuel rate for ground-test mock-up at constant values of blower pressure coefficient and engine speed.

The calculated cold static thrust as a function of the blower pressure coefficient is labeled "Engine only" in figure 4. The static thrusts shown correspond to maximum engine or blower conditions as indicated by the intersections of the curves in figure 3. The thrust at first rises markedly with increasing blower pressure. The increasing thrust is due to increasing engine power and to increasing blower and duct efficiencies. With still higher blower pressures, however, the increasing efficiency can no longer compensate for the loss of power and quantity flow with the result that the thrust tends to show a flat maximum and starts to decrease.

An extensive series of measurements of cold static thrust at various values of the blower pressure coefficient was made in order to establish a correlation between experimental and calculated results to be used in the prediction of flight performance. These tests indicated that a calculation such as that shown in appendix B gave values which checked with experiment within 5 percent over the blower-pressure range. One of these comparisons is indicated by the test points shown at zero fuel rate in figure 5.

Hot.—Thrust curves corresponding to the maximum engine and blower conditions shown in figure 3 with various fractions of the intake air burned and at various rates of fuel burning are given in figure 4. For large fractions of the air burned, the maximum thrust is seen to shift to higher blower pressures; thus the best results are obtained for high pressures and small quantity flows for which the blower is operating relatively near its stall.

In order to test the validity of calculations of the thrust due to burning (Meredith effect), comparisons, were made between calculated and measured thrust values over a range of fuel rates. The comparisons are shown in figure 5 as the variation in $\dfrac{\text{Static thrust}}{\rho}$ with the fuel rate at constant values of the blower pressure coefficient and engine speed. The value of $\dfrac{\text{Static thrust}}{\rho}$ was used because the thrust was found to vary linearly with ρ at the same pressure coefficient, fuel rate, and engine speed. The good agreement between experimental and calculated values is evident from figure 5.
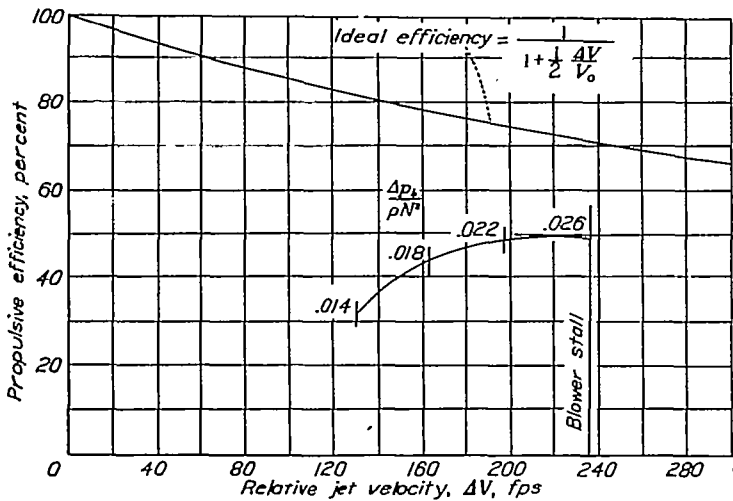
FIGURE 6.—Propulsive and ideal efficiency as functions of relative jet velocity for jet-propulsion system. Cruising flight at 200 miles per hour on engine only; altitude, 10,000 feet; constant thrust horsepower, 218.

The experimental values shown in figure 5 represent values from only one series of experiments. Other test data obtained from a previous series of tests with the blower engine-cooling blades set at a slightly different angle gave values of thrust as high as 2110 pounds. This value of thrust of 2110 pounds was attained at a blower coefficient $\Delta p_b/\rho N^2$ of 0.024, engine speed of 2150 rpm, and a fuel rate of 2.3 pounds per second. Other burning tests were made in which fuel rates up to 3 pounds per second were attained.

PERFORMANCE OF JET-PROPULSION SYSTEM

FLIGHT CONDITIONS

. Cold.—In order to investigate the cold cruising-flight condition—flight with engine alone—calculations were made, which gave the results shown in figure 6. The thrust horsepower was held constant at 218, which is considered to be approximately that required for level flight at 200 miles per hour and at an altitude of 10,000 feet for the jet-propulsion airplane (to be described later). The propulsive efficiency—the ratio of thrust horsepower to engine horsepower—was then plotted against the relative jet velocity ΔV that corresponds to varying blower conditions. The relative jet velocity ΔV is the difference between the jet velocity and the flight velocity. The ideal efficiency of a propulsion jet is also shown in figure 6. These results clearly indicate the optimum operating conditions and show that the improvement in blower-duct efficiency with increasing pressure more than compensates for the lower jet-propulsive efficiency.

The thrust attainable plotted against blower coefficient for cruising flight on engine only at a speed of 200 miles per hour and at 10,000 feet is shown in figure 7. It will be noted that the thrust rises markedly with increasing blower pressures.

Hot.—Results of calculated thrusts as a function of blower pressure coefficient for various fractions of the intake air burned and for various fuel rates at an altitude of 10,000 feet for high-speed flight conditions of 200, 400, and 600 miles per hour are presented in figures 7, 8, and 9, respectively. It is evident that, for the higher speeds, the best
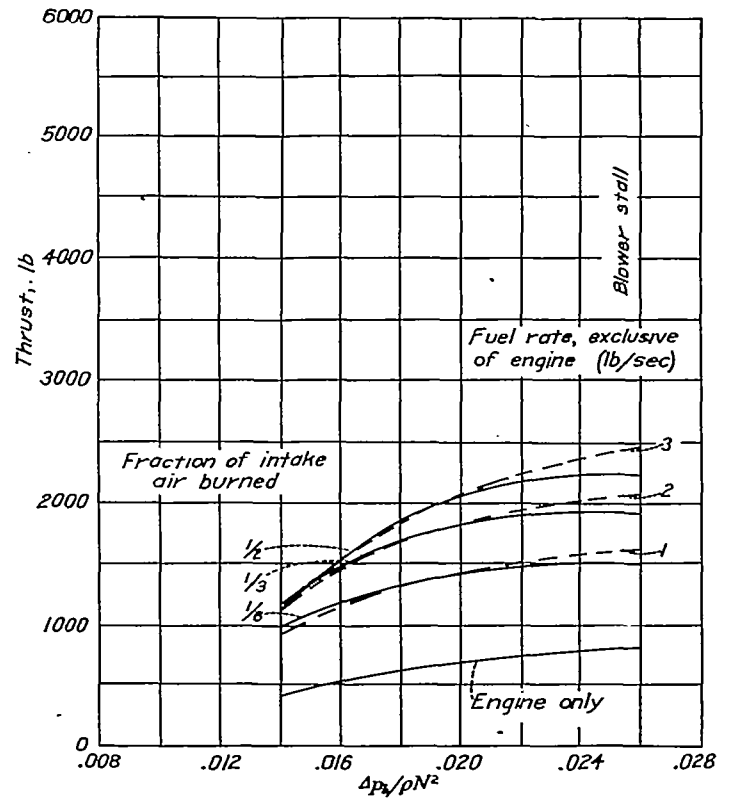

FIGURE 7.—Thrust as a function of blower pressure coefficient for jet-propulsion system. Various burning conditions and on engine only; flight at 200 miles per hour; altitude, 10,000 feet.
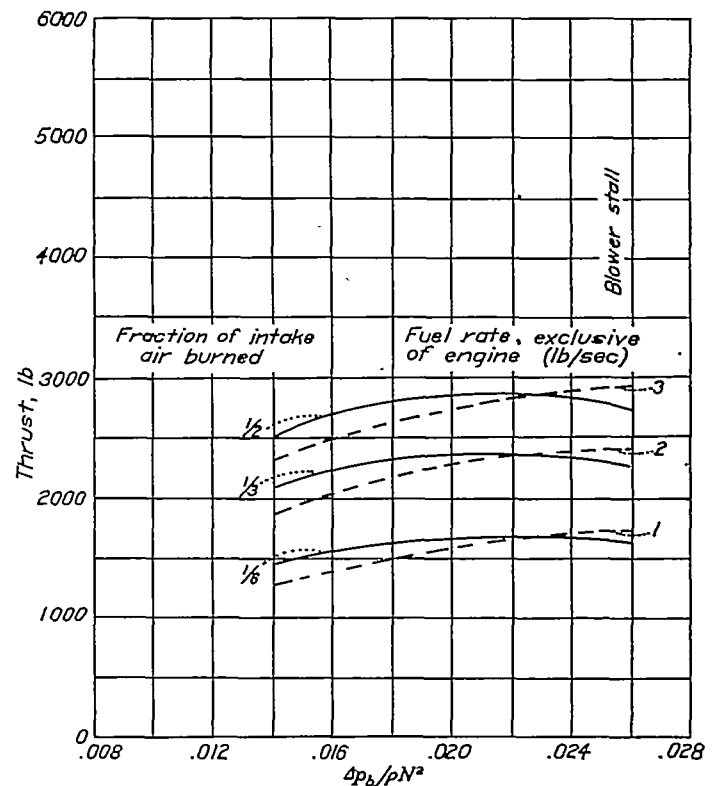

FIGURE 8.—Thrust as a function of blower pressure coefficient for jet-propulsion system. Various burning conditions; flight at 400 miles per hour; altitude, 10,000 feet.
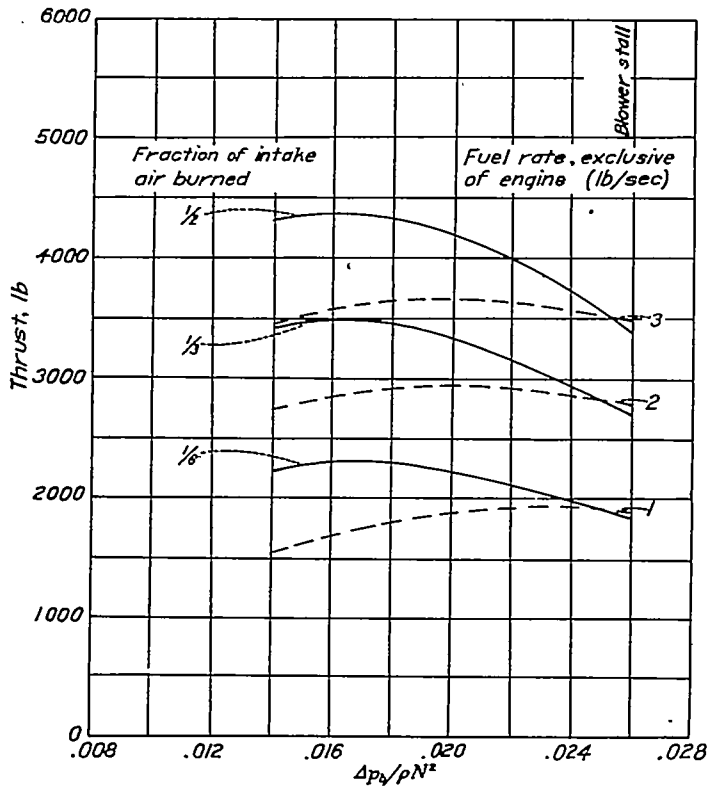
FIGURE 9.—Thrust as a function of blower pressure coefficient for jet-propulsion system. Various burning conditions; flight at 600 miles per hour; altitude, 10,000 feet.

results are no longer obtained at the highest blower pressures—particularly for the higher fractions and higher fuel rates, which show a maximum within the lower pressure range of the blower.

VARIATION IN NOZZLE-EXIT AREA

Calculations of the nozzle-exit areas by the method given in appendix B were found to check reasonably well with the actual nozzle areas for the tests for which data are shown in figure 5. The calculations generally tended to give slightly larger than the actual areas for the higher fractions of air burned and for the higher fuel rates. The somewhat larger areas indicated by calculations can probably be explained by the fact that complete mixing is assumed for the calculated areas. If mixing were complete, the mean temperatures would extend to the nozzle edges. Complete mixing, however, did not occur because a blanket of relatively cool air was maintained along the nozzle edges in order to keep the nozzle and surrounding structure at normal temperatures.

Results of calculations of nozzle-exit areas for some typical operating conditions as a function of the fraction of intake air burned are shown in figure 10. All the values shown are for an intermediate blower pressure coefficient $\Delta p_b/\rho N^2$ of 0.020 and for the highest engine power that can be obtained by loading the blower to the limiting engine manifold pressure or limiting engine speed. The maximum nozzle-exit area required is indicated at the highest fraction of the air burned for the static operating condition. The area shown could be reduced, however, by operating at a higher

blower pressure. It appears that the minimum nozzle-exit area required is for maximum speed on engine alone at sea level.

The foregoing results indicate that a nozzle exit of variable area would be desirable for a practical application of the jet-propulsion system investigated. The absolute necessity for a continuously adjustable nozzle is not indicated, however, because an examination of the area variation will show that as few as three area settings will enable the system to operate over a wide range of flight conditions close to optimum.

THE EXPERIMENTAL AIRPLANE AND PERFORMANCE PREDICTIONS

The experimental airplane represented by the ground-test mock-up was originally designed, without the benefit of ground-test data, to represent a reasonably close approach to the optimum. The airplane was designed to use the same propulsion unit as that used in the ground-test mock-up. A cross section through the fuselage of the airplane studied is given in figure 11; the cockpit, the landing gear, and details of the power plant are shown. The wing was selected from considerations of gasoline volume available in the wing and structural practicability. Early in the study it became apparent that wing weight and therefore wing structural efficiency were of prime importance; hence, a rather thorough wing analysis was made to select the optimum. The analysis included studies of a series of wings of various areas, aspect ratios, and thickness ratios.
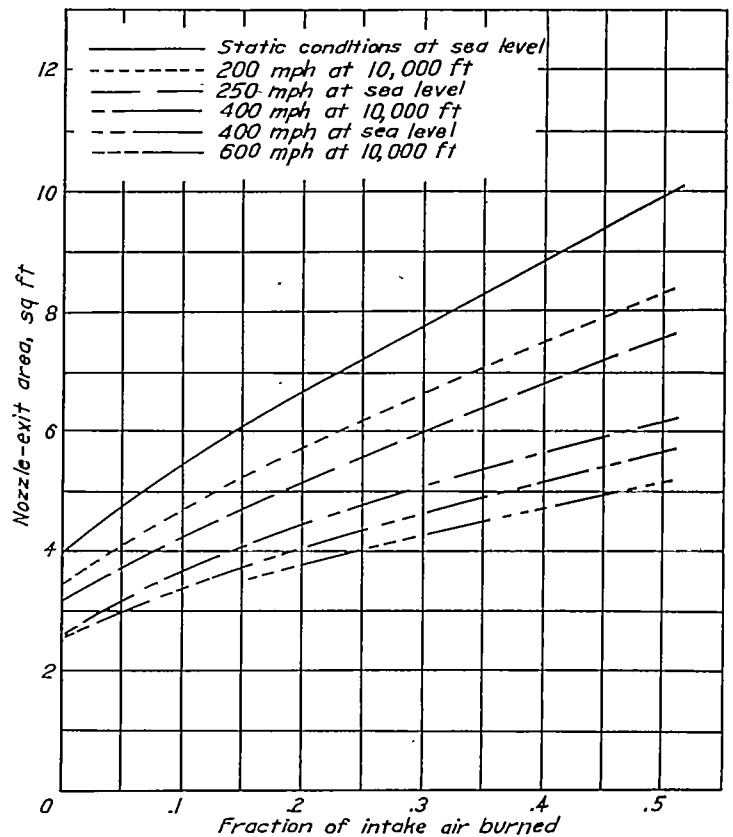

FIGURE 10.—Nozzle-exit area as a function of fraction of intake air burned for jet-propulsion system at various operating conditions. $\Delta p_b/\rho N^2$, 0.020.

1	Nose air intake	25	23 gas-vapor jets
2	Inner cone	26	Main landing gear
3	Nose-wheel well	27	Mixing duct
4	Nose wheel	28	Main boiler pancake section
5	Intersection well and cone	29	Spark igniter for annular igniter
6	Flight controls	30	Annular igniter
7	Instrument space	31	Main combustion chamber
8	Radio	32	Tail bumper
9	Nose-gear retraction	33	Variable-area nozzle
10	Transformers for spark igniters	34	Vee-tail
11	Oil tank	35	Wing carry-through truss
12	Batteries	36	Wing root section
13	Blower main stages	37	Canopy
14	Blower engine-cooling stage	38	CO_2 extinguisher
15	Engine-cooling duct	39	Duct-surface oil cooler
16	P. & W. R-1535 Twin Wasp, Jr., engine	40	Turn-over pylon
17	Main air duct	41	Engine controls
18	Engine mounting ring	42	Instrument board
19	Exhaust boilers for primary fire	43	Intersection pilot's well and cone
20	Fuel pump	44	Pilot's well
21	Primary burner	45	Transparent section
22	Spark igniter for primary fire	46	Burning control
23	Fuselage gasoline	47	Floor
24	Main boiler spiral section		

Main landing gear and
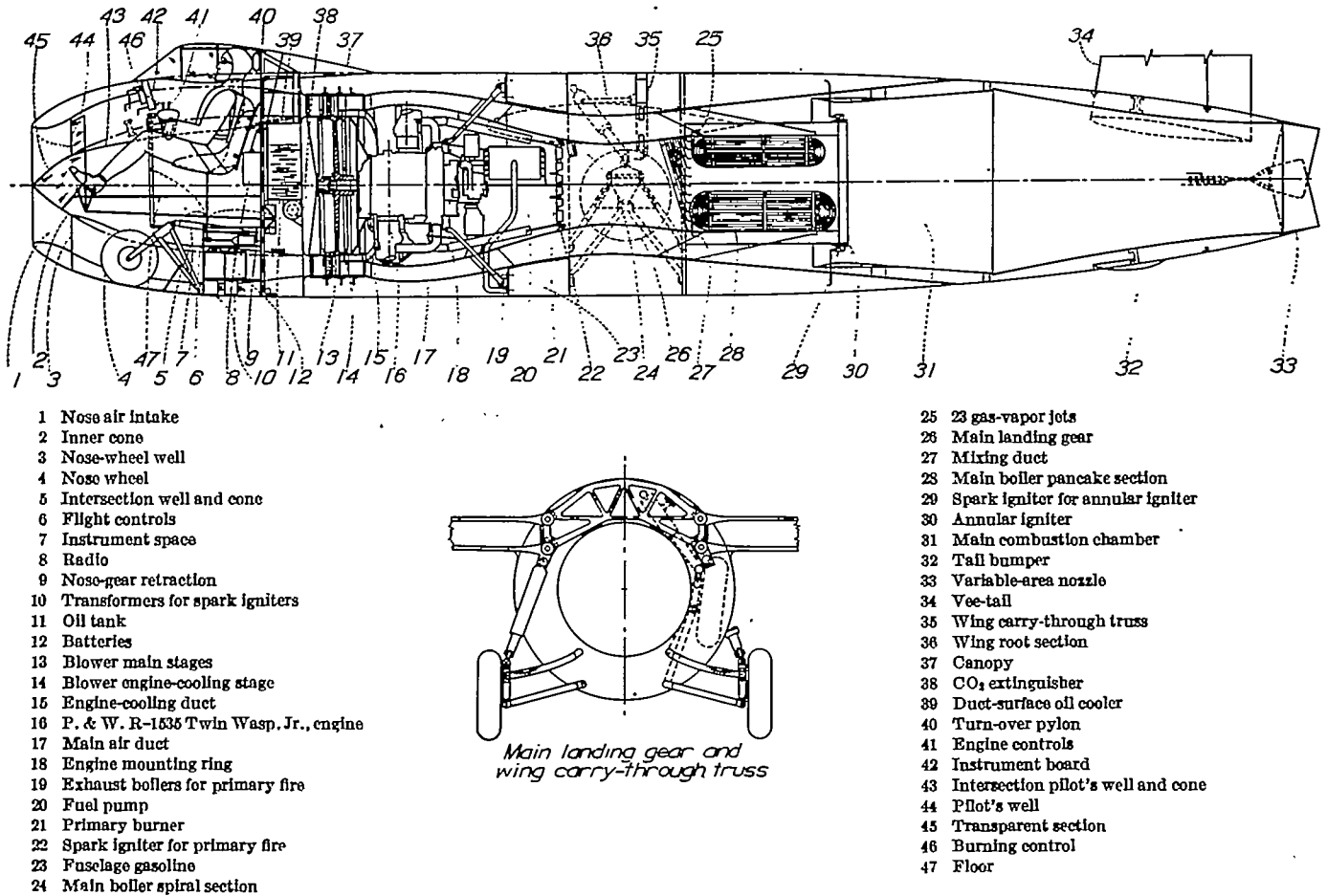wing carry-through truss

FIGURE 11.—Section through experimental jet-propulsion airplane.

The drag estimate for the airplane was made from the following considerations: The high critical speeds desired require smooth and careful construction. Owing to the general cleanness of the design and the absence of disturbing slipstream effects, it is assumed that wind-tunnel data on smooth models may be directly applied to the prototype. Finally, the use of low-drag wings and full-span flaps allows the airplane to maintain low drags up to lift coefficients corresponding to the maximum lift-drag ratio L/D. The profile-drag coefficient for the experimental airplane was therefore estimated to be 0.0153. It should nevertheless be realized that unusually careful construction methods would be necessary to obtain such drags on the airplane, comparable with those from tests of smooth models. A weight breakdown of the airplane and some dimensions and performance parameters are as follows:

Weight, pounds
Wing, including tanks_____ 1580
Tail group_____ 137
Fuselage, including ducts and integral gas tank_____ 1460
Power plant_____ 2363
    Engine, including starter, generator, controls,
    engine mount, exhaust boilers, and primary
    burner_____ 1388
    Main burner, including boiler_____ 400
    Blower_____ 575

Landing gear_____ 637
Instruments, pilot's seat, controls, and furnishings_____ 160
Pilot, parachute, radio, battery, and fire extinguisher____ 313
Oil tank_____ 35
Gasoline and oil_____ 3095

Gross weight, pounds_____ 9780

Wing area, square feet_____ 215
Wing span, feet_____ 41.4
Wing thickness ratio_____ 0.15
Taper ratio_____ 3:2
Estimated airplane drag coefficient_____ 0.0153
Maximum L/D_____ 19.5

It may be noted in figure 11 that a vee-tail is specified. This type of tail was selected to minimize the tail drag and to avoid compressibility disturbances from the canopy and wing wake after the shock. Tests in the NACA two-dimensional low-turbulence pressure tunnel comparing the drags of a vee-tail and a conventional tail indicated appreciably lower drags for the vee-tail. Stability tests of a complete 0.193-scale powered model of the experimental airplane in the LMAL 7- by 10-foot tunnel indicated, within the power range of the model, satisfactory stability characteristics for the combination with the vee-tail. The two tails tested were designed to give the same stability characteristics for purposes of comparison and neither tail necessarily represents the optimum for the airplane.

The most important results are presented in figure 12 as curves of power available and estimated power required for flight at an altitude of 10,000 feet. The power-available curves represent values for a blower pressure coefficient $\Delta p_b/\rho N^2$ of 0.020 obtained from the curves of figures 7 to 9, which therefore give the highest engine power that can be absorbed by the blower as limited by the engine manifold pressure or engine speed. The engine is assumed to be supercharged to deliver full power at 10,000 feet.

It is evident that large excess powers may be obtained even for the highest speeds at which the power-required curve
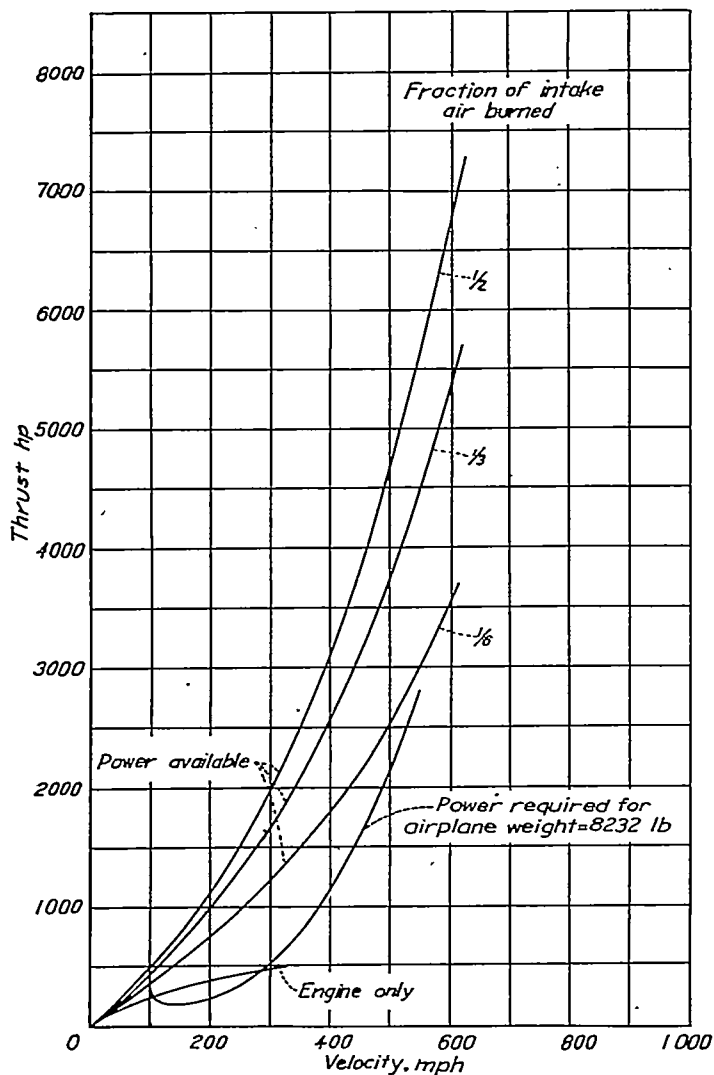
FIGURE 12.—Power available and estimated power required for experimental jet-propulsion airplane with various fractions of intake air burned and with engine only. Altitude, 10,000 feet; $\Delta p_b/\rho N^2$, 0.020.

may be considered fairly well established. This curve terminates at 550 miles per hour owing to uncertainties in the quantitative drag values above the speed of the compressibility burble. The maximum speeds therefore cannot be estimated.

The results shown in figure 12 certainly indicate that this type of jet-propulsion airplane has unusual capabilities in the high-speed range above that of conventional airplanes. It is evident that the thrust horsepower developed by the jet-propulsion system tends to increase rapidly with speed,

rather than to decrease with speed as for the conventional engine-propeller-driven airplane. A comparison of the fuel rate of the jet-propulsion system with a hypothetical conventional airplane proves interesting. If it is assumed (fig. 12) that some increase in power is required above that shown at the critical speed of 550 miles per hour, the power required for the jet-propulsion airplane to maintain flight at this speed falls about on the curve for one-sixth of the air burned and has a value of 2980 thrust horsepower. Cross plots of the fuel rates shown in figures 7 to 9 indicate a fuel rate of 1.21 pounds per second for this condition. From these values, the thrust-horsepower specific fuel consumption for level flight at 550 miles per hour at 10,000 feet is then 1.46 pounds per thrust horsepower-hour. If the hypothetical conventional airplane had a brake-horsepower specific fuel consumption of 1.0 pound per brake horsepower-hour and a propulsive efficiency of 0.685, the fuel rates would be the same. The conventional airplane, however, is hypothetical and any quantitative estimates of fuel consumption and efficiencies remain uncertain.

It therefore appears that the extreme power-output capabilities of the jet-propulsion system are limited mainly by the speeds at which it is practicable to fly the airplane. If, for the experimental jet-propulsion airplane, it were considered expedient to hold the speed below 550 miles per hour at 10,000 feet, the maximum power would be limited by the fraction of air that could be burned and by the quantity of fuel that could be supplied to the combustion chamber. At this speed, the curve in figure 12 representing one-half the air burned corresponds to a burning rate of 3.64 pounds per second and, at the same speed for one-third the air burned, the fuel rate is 2.42 pounds per second. From the burning experiments described herein, it was found that the system could burn one-half the intake air up to a fuel rate of 3 pounds per second. This value of 3 pounds per second, however, does not necessarily represent the maximum fuel rate attainable. It may be stated, therefore, that the system is capable of developing the horsepower corresponding to a fuel rate of 3 pounds per second (5050 thp at 550 mph)— certainly an outstanding accomplishment for a power plant of the size and weight indicated by the ground-test mock-up.

In order to estimate the possibilities of utilizing the large excess powers indicated, an investigation of the rates of climb of the experimental airplane was made. Results of this study for altitudes up to 50,000 feet are shown in table I and in figure 13. All values of power available were calculated for the limiting blower or engine conditions at a blower pressure coefficient $\Delta p_b/\rho N^2$ of 0.020 and an airplane weight of 8232 pounds, which represents the weight of the experimental airplane with one-half its maximum fuel load. The changes in slope of the curves in figure 13 are due to the change in limiting blower load with increasing altitude. Up to altitudes just higher than 10,000 feet for the two higher fractions of air burned, the airplane is climbing at its critical speed, with the attendant high intake-air densities. These high densities load the blower to the limiting engine manifold pressure and the engine speed increases up to this altitude. At higher altitudes, however, the blower is held to the limiting speed that causes the mass flow through the

system to decrease with altitude. The excess power available consequently decreases with increasing altitude above the point where the blower limitation changes. On the curve for one-sixth of the air burned and for climb on engine only, this change occurs somewhat below 10,000 feet owing to the lower intake-air densities at the lower speeds of climb.

The flight-path climbing velocities shown in table I indicate increases in climbing velocity with increases in altitude when one-sixth of the air is burned; the climbing velocity finally reaches the airplane critical speed at about 40,000
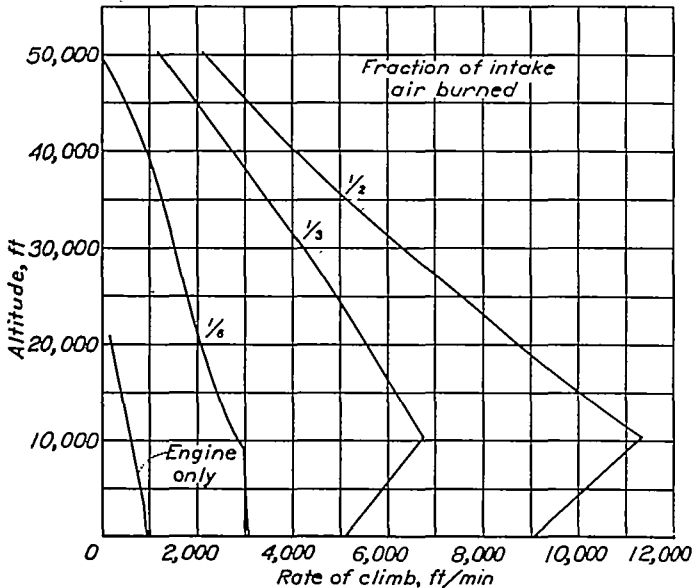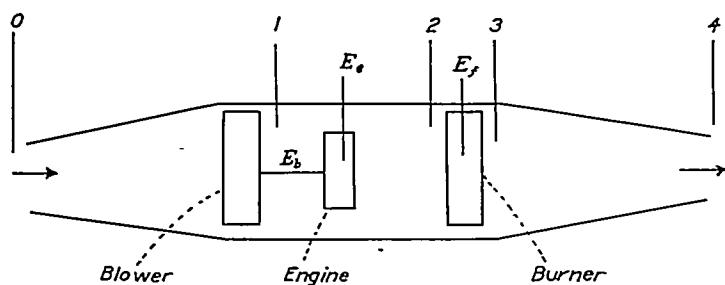

FIGURE 13.—Rates of climb for experimental jet-propulsion airplane at various altitudes. $\Delta p_t/\rho N^2$, 0.020; weight of airplane, 8232 pounds.

feet. The same is generally true for climb when one-third of the air is burned, except that the airplane critical speed is reached at about 10,000 feet. The maximum rates of climb indicated for burning one-half the air are at the airplane critical speed for all the altitudes. The fact that the maximum rates of climb occur at the highest airplane speed for the higher fractions of air burned may be seen in figure 12 by noting the divergence of the power-available and power-required curves for one-third and one-half of the air burned.

The high rates of climb indicated again suggest interesting possibilities for an airplane utilizing the system investigated.

The range of the experimental airplane at an altitude of 10,000 feet and using all its fuel for cruising on engine only is estimated to be 2770 miles. If only one-half the total fuel is used for cruising, the range is estimated to be 1300 miles. The gasoline left could then be used for high performance at a fuel rate of 3 pounds per second for 8.6 minutes or 25.8 minutes at a fuel rate of 1 pound per second.

CONCLUSIONS

Experiments conducted with the NACA jet-propulsion ground-test setup indicated the following conclusions:

1. The main fire could be restricted to an intense, small, and short annular blue flame burning steadily and under control in the intended combustion space. It was possible with these conditions to maintain a blanket of cool air between the hot gases and the combustion chamber and nozzle walls. Furthermore, adequate cooling air might readily be provided in order to carry away any radiant heat and to maintain the walls and structure at normal temperatures.

2. The system investigated was capable of burning almost one-half of the air taken in at the nose up to fuel rates of 3 pounds per second.

3. Calculations may be expected to give reasonably accurate results for flight-performance predictions.

4. The basic features of the jet-propulsion system investigated in the ground-test mock-up were sufficiently developed to be considered applicable to flight installation. Calculations indicated that an airplane utilizing this system would have unusual capabilities in the high-speed range above the speeds of conventional aircraft and would, in addition, have moderately long cruising ranges if only the engine were used.

APPENDIX A

COMPRESSION-RATIO. ANALYSIS

An expression is derived for thermopropulsive efficiency in terms of compression ratio and other basic parameters for the system shown in the following diagrammatic sketch:

The results of the compression-ratio analysis are presented in figures 14 to 16. In the system analyzed, the atmospheric air is compressed by dynamic action and a blower, which is driven by an engine or prime mover of fixed thermal efficiency. In addition to the waste heat energy of the engine, heat is added to the stream by a gasoline burner or similar device. The heated and compressed air is then expanded

FIGURE 15.—Effect of blower-duct efficiency and ratio of burner heat input to engine heat input on variation of thermopropulsive efficiency with effective compression ratio. $C_T=1.30; \eta_e=0.35$.

through a nozzle to atmospheric pressure, and the resulting total momentum change produces a thrust.

The simplifying assumptions made for this analysis are as follows:

    (a) No energy losses through the walls

    (b) Complete combustion in the intended regions

    (c) Stagnation conditions in the combustion chamber and no nozzle losses

    (d) A blower-duct efficiency η_b that includes duct and blower losses back to station 2

    (e) Constant specific heat throughout the system

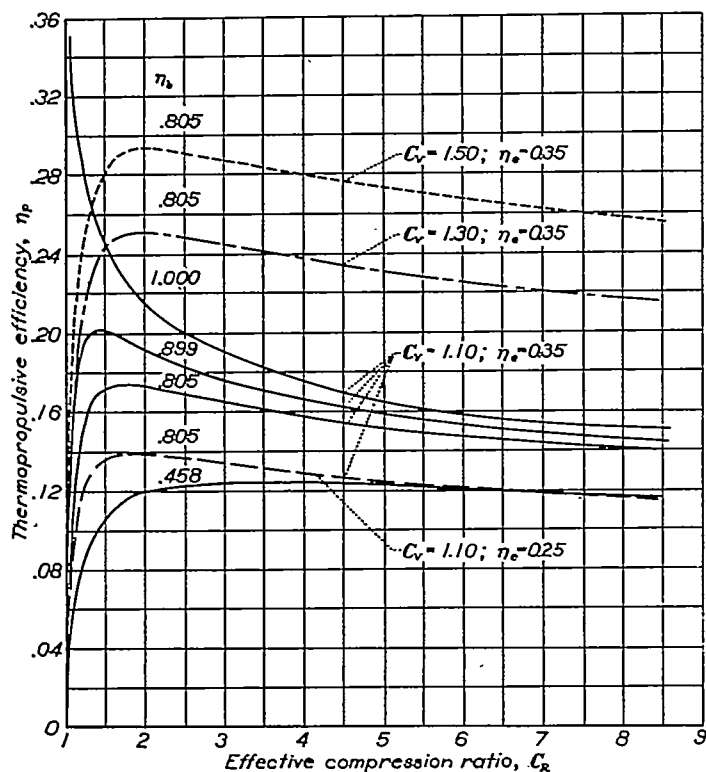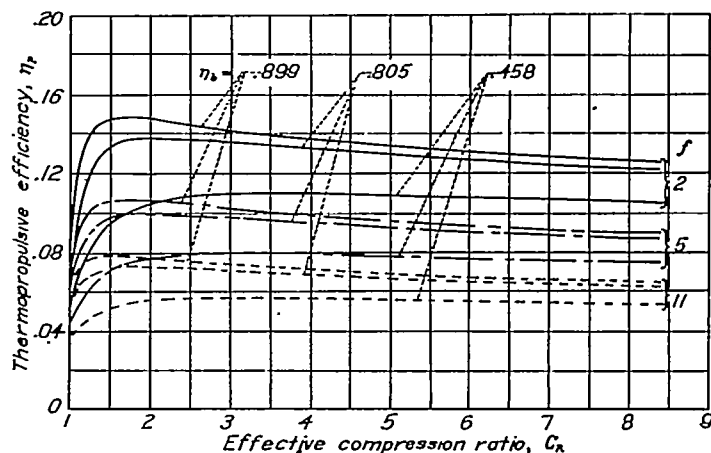   (f) Mass of the fuel neglected

FIGURE 14.—Effect of blower-duct efficiency, dynamic compression ratio, and engine thermal efficiency on variation of thermopropulsive efficiency with effective compression ratio. $f=0$.
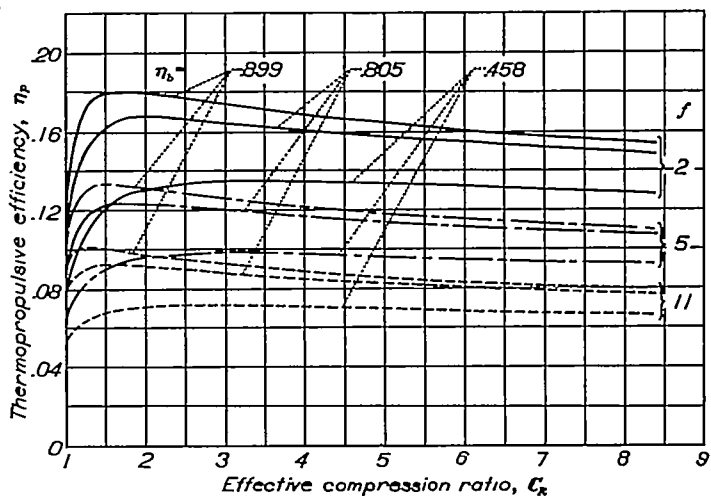

FIGURE 16.—Effect of blower-duct efficiency and ratio of burner heat input to engine heat input on variation of thermopropulsive efficiency with effective compression ratio. $C_T=1.50; \eta_e=0.35$.

502

The thermopropulsive efficiency η_p is defined as the ratio of thrust power to the total fuel energy input:

$$\eta_p = \frac{\text{Thrust} \times \text{Flight velocity}}{\text{Total fuel energy input}}$$

$$= \frac{(V_4 - V_0)V_0}{E_e + E_f} \qquad (1)$$

where

E_e total energy input to engine per unit mass of air

E_f total energy input to burner per unit mass of air

The quantity V_0 in terms of the dynamic compression ratio $\frac{p_{0t}}{p_0}$ from Bernoulli's equation is

$$V_0 = \sqrt{2c_p T_{0t}\left[1 - \left(\frac{p_0}{p_{0t}}\right)^{\frac{\gamma-1}{\gamma}}\right]}$$

For simplicity, the dynamic compression ratio is denoted by the symbol C_V; hence

$$V_0 = \sqrt{2c_p T_{0t}\left[1 - C_V^{-\frac{\gamma-1}{\gamma}}\right]}$$

Now

$$V_4 = \sqrt{2c_p T_{3t}\left[1 - \left(\frac{p_0}{p_{3t}}\right)^{\frac{\gamma-1}{\gamma}}\right]}$$

but

$$\frac{p_0}{p_{3t}} = \frac{1}{C_V C_R}$$

where C_R is the effective compression ratio at station 2, or

$$C_R = \frac{p_{2t}}{p_{0t}}$$

It follows that

$$V_4 = \sqrt{2c_p T_{3t}\left[1 - (C_V C_R)^{-\frac{\gamma-1}{\gamma}}\right]} \qquad (2)$$

Now

$$T_{3t} = T_{0t} + \Delta T_{0t,\,2t} + \Delta T_{2t,\,3t} \qquad (3)$$

and

$$\Delta T_{2t,\,3t} = \frac{E_f}{c_p}$$

$$= f\frac{E_e}{c_p}$$

where

$$f = \frac{E_f}{E_e}$$

but

$$\Delta T_{0t,\,2t} = \frac{E_e}{c_p}$$

hence

$$\Delta T_{0t,\,2t} + \Delta T_{2t,\,3t} = (1+f)\frac{E_e}{c_p}$$

If

$$E_b = \frac{\text{Shaft power}}{\text{Unit mass of air}}$$

$$= \eta_e E_e$$

where η_e is the thermal efficiency of the engine, and if

$$E_b = c_p \Delta T_{0t,\,1t} = c_p T_{0t}\left(\frac{T_{1t}}{T_{0t}} - 1\right)$$

where $\Delta T_{0t,\,1t}$ is the stagnation-temperature rise across the blower, then

$$E_e = \frac{c_p T_{0t}\left(\frac{T_{1t}}{T_{0t}} - 1\right)}{\eta_e} \qquad (4)$$

If adiabatic conditions of flow existed in the blower-duct system, the temperature ratio T_{1t}/T_{0t} would produce a compression ratio higher than that actually attainable and also exactly equal to $\left(\frac{T_{1t}}{T_{0t}}\right)^{\frac{\gamma}{\gamma-1}}$. The ratio of the actual compression ratio C_R to this adiabatic compression ratio is defined as the blower-duct efficiency η_b; therefore

$$\eta_b = \frac{C_R}{\left(\frac{T_{1t}}{T_{0t}}\right)^{\frac{\gamma}{\gamma-1}}}$$

and

$$\frac{T_{1t}}{T_{0t}} = \left(\frac{C_R}{\eta_b}\right)^{\frac{\gamma-1}{\gamma}}$$

Substituting in equation (4) gives

$$E_e = \frac{c_p T_{0t}\left[\left(\frac{C_R}{\eta_b}\right)^{\frac{\gamma-1}{\gamma}} - 1\right]}{\eta_e} \qquad (5)$$

and, from equation (3),

$$T_{3t} = T_{0t} + (1+f)\frac{T_{0t}\left[\left(\frac{C_R}{\eta_b}\right)^{\frac{\gamma-1}{\gamma}} - 1\right]}{\eta_e}$$

Substituting in equation (2) yields

$$V_4 = \sqrt{2c_p T_{0t}\left[1 - (C_V C_R)^{-\frac{\gamma-1}{\gamma}}\right]\left\{1 + \frac{1+f}{\eta_e}\left[\left(\frac{C_R}{\eta_b}\right)^{\frac{\gamma-1}{\gamma}} - 1\right]\right\}}$$

The numerator, or output term, of equation (1) may now be evaluated as follows:

$$(V_4-V_0)V_0=2c_pT_1\left[\sqrt{\left[1-(C_VC_R)^{-\frac{\gamma-1}{\gamma}}\right]\left\{1+\frac{1+f}{\eta_c}\left[\left(\frac{C_R}{\eta_b}\right)^{\frac{\gamma-1}{\gamma}}-1\right]\left[1-C_V^{-\frac{\gamma-1}{\gamma}}\right]\right\}}-\left(1-C_V^{-\frac{\gamma-1}{\gamma}}\right)\right] \tag{6}$$

From the foregoing equations the energy input is

$$E_e+E_f=(1+f)E_e$$

Thus, from equation (5),

$$E_e+E_f=(1+f)\,c_pT_{0f}\frac{\left[\left(\frac{C_R}{\eta_b}\right)^{\frac{\gamma-1}{\gamma}}-1\right]}{\eta_c} \tag{7}$$

By use of equations (6) and (7), equation (1) may be expressed as

$$\eta_p=2\eta_c\left\{\frac{\sqrt{\left\{1+\frac{1+f}{\eta_c}\left[\left(\frac{C_R}{\eta_b}\right)^{\frac{\gamma-1}{\gamma}}-1\right]\right\}\left[1-(C_VC_R)^{-\frac{\gamma-1}{\gamma}}\right]}\left(1-C_V^{-\frac{\gamma-1}{\gamma}}\right)-\left(1-C_V^{-\frac{\gamma-1}{\gamma}}\right)}{\left[\left(\frac{C_R}{\eta_b}\right)^{\frac{\gamma-1}{\gamma}}-1\right](1+f)}\right\}$$

APPENDIX B

SAMPLE CALCULATION

For a sample calculation of available power from the jet-propulsion system, a velocity of 600 miles per hour at an altitude of 10,000 feet is selected. The fraction of air burned is taken as one-half and the blower pressure coefficient $\Delta p_b/\rho N^2$, as 0.022.

In order to obtain conditions at the blower equivalent to static-test conditions, the following values are taken from compressible-flow considerations with the subscripts 0 for atmospheric conditions and i for impact conditions:

$$p_i = p_0\left(1 + \frac{\gamma-1}{2}M_0^2\right)^{\frac{\gamma}{\gamma-1}}$$

$$= 1455.7[1 + (0.2)(0.818)^2]^{3.5}$$

$$= 2261 \text{ lb/sq ft}$$

$$T_i = T_0\left(\frac{p_i}{p_0}\right)^{\frac{\gamma-1}{\gamma}}$$

$$= 483\left(\frac{2261}{1455.7}\right)^{0.286}$$

$$= 548° \text{ F abs.}$$

$$\rho_i = \rho_0 \frac{p_i}{p_0}\frac{T_0}{T_i}$$

$$= 0.00176 \frac{2261}{1455.7}\frac{483}{548}$$

$$= 0.002410 \text{ slug/cu ft}$$

The internal flows may then be considered equivalent to a static-ground condition having outside air conditions given by p_i, T_i, and ρ_i, and the same value of the blower pressure coefficient $\frac{\Delta p_b}{\rho N^2}=0.022$. This value is taken as the value of the independent variable (fig. 2) to represent a suitable blower-operating point.

From the blower-duct test curves (fig. 2), the values of $P/\rho N^3$ are used to plot blower power absorbed against engine speed for the air density involved in each case (fig. 17). The intersection of these curves with the curve of maximum engine power available or with the limiting engine speed gives the power output and speed of the engine for the different values of the blower pressure coefficient. From figure 17 for $\frac{\Delta p_b}{\rho N^2}=0.022$, the engine output is 1006 horsepower at 2530 rpm. From figure 2, then,
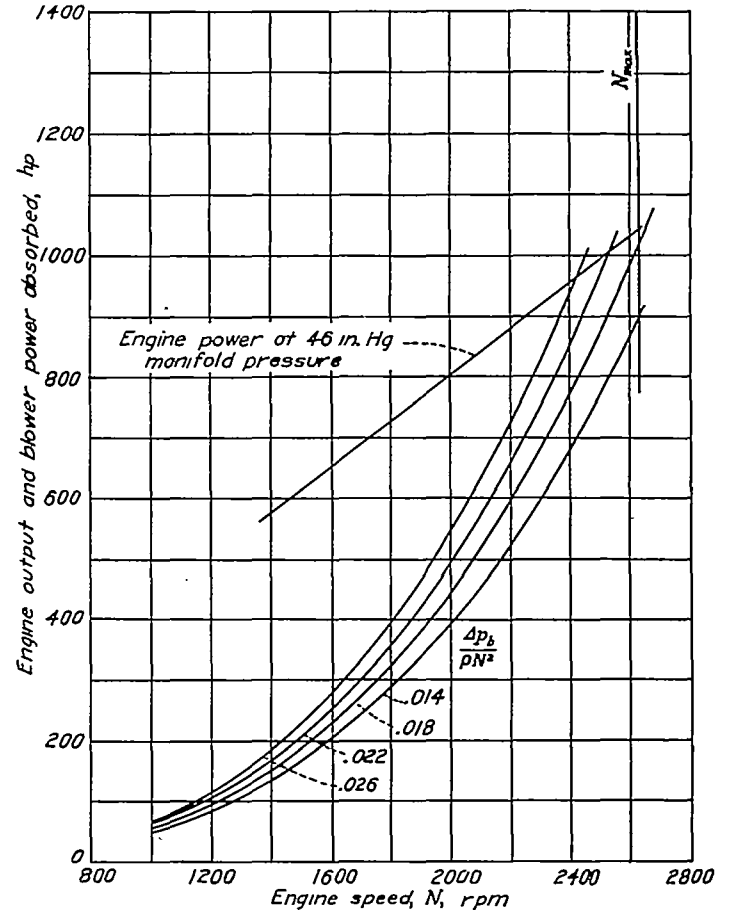
$$\frac{Q}{N}=0.533$$

FIGURE 17.—Engine output and blower power absorbed for jet-propulsion system in flight at 600 miles per hour at 10,000 feet. $\rho=0.002410$.

Hence,

$$Q = (0.533)(2530)$$

$$= 1348 \text{ cu ft/sec}$$

Available pressures for the jet are measured at station 2 in the combustion chamber and are represented in figure 2 as $\Delta p_2/\rho N^2$. These values represent the blower-pressure rise minus losses in pressure in the ducts between the blower and the large-area section where gasoline vapor is assumed to be introduced before burning occurs. An effective section area at this station of $A_2=13.2$ square feet is assumed. This area is estimated from considerations of variations in velocity across the section.

Station 3 is defined as a hypothetical station after burning has taken place and is assumed to have the same area as station 2. If the assumption that these areas are equal is followed, the law of conservation of momentum between the stations may be written as

$$p_2A_2+M=p_3A_3+m_3V_3$$

505

where M represents the momentum at station 2 of the gas and air flowing into the combustion chamber. From this relation, it may be shown that

$$p_3 = \frac{p_2 + \frac{M}{A} + \sqrt{\left(p_2 + \frac{M}{A}\right)^2 - 4\frac{M}{A}p_2\frac{T_3}{T_2}}}{2}$$

The terms in this equation will be evaluated in order that the equation may be employed to find the available pressure p_3 in the combustion chamber after burning.

$$\frac{\Delta p_2}{\rho N^2} = 0.01602$$

$$\Delta p_2 = (0.01602)(0.002410)(2530)^2$$

$$= 247 \text{ lb/sq ft}$$

$$p_2 = p_i + \Delta p_2$$

$$= 2261 + 247$$

$$= 2508 \text{ lb/sq ft}$$

The temperature rise at station 2 may be obtained by considering that the engine adds the equivalent heat of all the fuel it consumes. The temperature rise then is

$$\Delta T_2 = \frac{H}{c_p g \rho_i Q}$$

where H is the heat equivalent of the fuel in Btu per second. If a specific fuel consumption for the engine of 0.6 pound per brake horsepower-hour and a heating value of gasoline of 18,700 Btu per pound is assumed, the temperature rise of the air is

$$\Delta T_2 = \frac{\frac{(1006)(0.6)(18700)}{3600}}{(0.24)(32.2)(0.002410)(1348)}$$

$$= 125° \text{ F}$$

Then

$$T_2 = T_i + \Delta T_2$$

$$= 548 + 125$$

$$= 673° \text{ F abs.}$$

In order to burn one-half the air passing through the system, the fuel burning rate for this case is

$$F_R = \rho_i Q g \left(\frac{1}{15}\right)\left(\frac{1}{2}\right)$$

$$= (0.002410)(1348)(32.2)\left(\frac{1}{15}\right)\left(\frac{1}{2}\right)$$

$$= 3.49 \text{ lb/sec}$$

where it is assumed that the mass of air required for complete combustion of the gasoline is 15 times the mass of gasoline.

The temperature rise from stations 2 to 3 for a gasoline burning rate of 3.49 pounds per second is

$$\Delta T_{2,3} = \frac{H}{c_p g m_3}$$

where c_p is the heat-capacity coefficient for exhaust gases taken from figure 18 for an initially estimated T_3 by interpolating between the two curves for the fraction of air burned.
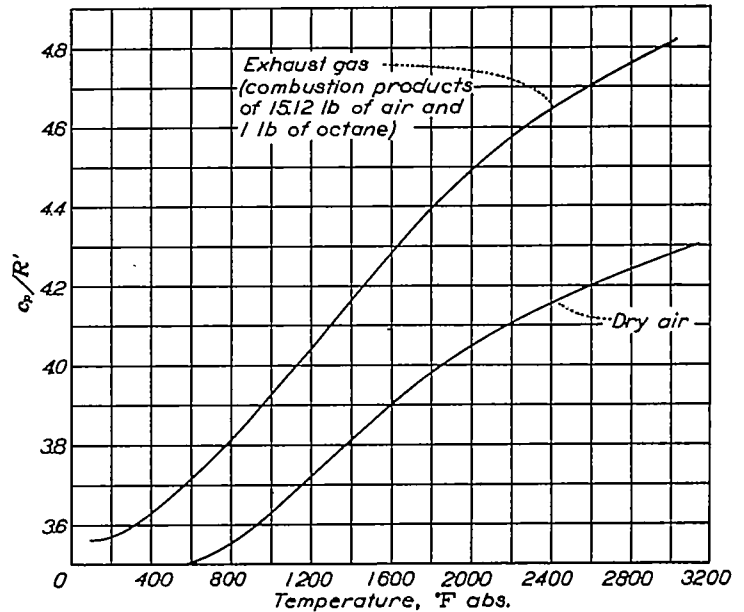

FIGURE 18.—Variation with temperature of ratio of heat-capacity coefficient to gas constant for air and exhaust gas.

If T_3 is estimated to be 2635,

$$\frac{c_p}{R'} = 4.462$$

$$c_p = \frac{c_p}{R'}(0.069)$$

$$= (4.462)(0.069)$$

$$= 0.3079 \text{ Btu/lb/°F}$$

and

$$m_3 = \rho_i Q + m_{gas}$$

$$= 3.357 \text{ slugs/sec}$$

Then

$$\Delta T_{2,3} = \frac{(18700)(3.49)}{(0.3079)(32.2)(3.357)}$$

$$= 1961° \text{ F}$$

$$T_3 = T_2 + \Delta T_{2,3}$$

$$= 673 + 1961$$

$$= 2634° \text{ F abs.}$$

These steps are repeated until the final T_3 is close to the estimated T_3.

The momentum M entering at station 2 is

$$M = M_{gas} + M_{air}$$

$$= m_{gas}(763) + \frac{m_{air}^2 R T_2}{P_2 A}$$

where
$$m_{gas}=\frac{3.49}{32.2}$$
$$=0.1084 \text{ slug/sec}$$

and
$$m_{air}=\rho_i Q$$
$$=(0.002410)(1348)$$
$$=3.249 \text{ slugs/sec}$$

The velocity of the gasoline vapor in the jets is taken as 763 feet per second; the velocity of sound in the superheated vapor, at an estimated mean temperature of 800° F.

$$R=\frac{49,720}{28.72}$$
$$=1731 \text{ ft-lb/slug/°F}$$

where 28.72 is the molecular weight of air and exhaust gases. Then

$$M=(0.1084)(763)+\frac{(3.249)^2(1731)(673)}{(2508)(13.2)}$$
$$=83+371$$
$$=454 \text{ lb}$$

$$\frac{M}{A}=34.4 \text{ lb/sq ft}$$

and, finally,

$$p_3=\frac{2508+34.4+\sqrt{(2508+34.4)^2-(4)(34.4)(2508)\left(\frac{2634}{673}\right)}}{2}$$
$$=2402 \text{ lb/sq ft}$$

The velocity at station 3 may now be found as

$$V_3=\frac{m_3 R T_3}{A p_3}$$
$$=\frac{(3.357)(1731)(2634)}{(13.2)(2402)}$$
$$=483 \text{ ft/sec}$$

The jet velocity may be calculated from the familiar compressible-flow relation for the expansion from p_3 to p_0:

$$V_4'^2=V_3^2+2R\frac{c_p}{R'}T_3\left[1-\left(\frac{p_0}{p_4}\right)^{\frac{R'}{c_p}}\right]$$

$$V_4'^2=(483)^2+(2)(1731)(4.462)(2634)\left[1-\left(\frac{1455.7}{2402}\right)^{0.2241}\right]$$

$$=233,300+4,325,200$$

$$=4,558,500$$

$$V_4'=2135 \text{ ft/sec}$$

If a nozzle velocity efficiency of 0.95 is assumed,

$$V_4=0.95V_4'$$
$$=(0.95)(2135)$$
$$=2028 \text{ ft/sec}$$

The thrust is now

$$\text{Thrust}=m_{gas}V_4+m_{air}(V_4-V_0)$$
$$=(0.1084)(2028)+3.249(2028-880)$$
$$=3950 \text{ lb}$$

and the thrust horsepower is

$$\text{thp}=\frac{(3950)(880)}{550}$$
$$=6320 \text{ hp}$$

The nozzle-exit area is

$$A_4=\frac{m_3 R T_4}{p_0 V_4}$$

where

$$T_4=T_3-\Delta T_{3,4}$$
$$=T_3-T_3\left[1-\left(\frac{p_0}{p_3}\right)^{\frac{R'}{c_p}}\right]$$
$$=2634-280$$
$$=2354° \text{ F abs.}$$

Then

$$A_4=\frac{(3.357)(1731)(2354)}{(1455.7)(2028)}$$
$$=4.63 \text{ sq ft}$$

REFERENCE

1. Buckingham, Edgar: Jet Propulsion for Airplanes. NACA Rep No. 159, 1923.

TABLE I

FUEL RATES, NOZZLE-EXIT AREAS, AND ENGINE SPEEDS CORRESPONDING TO RATES OF CLIMB IN FIGURE 13

$$\left[\frac{\Delta p_b}{\rho N^2}=0.020\right]$$

Altitude (ft)	Fraction of intake air burned	Flight-path velocity (mph)	Fuel rate (exclusive of engine) (lb/sec)	Nozzle-exit area (sq ft)	Engine speed (rpm)
Sea level	Engine only	160	-------	3.52	2,600
	1/6	275	1.30	4.65	2,535
	1/4	410	2.90	4.70	2,440
	1/2	572	4.36	4.51	2,300
10,000	Engine only	185	-------	3.41	2,630
	1/6	335	1.05	4.47	2,630
	1/4	550	2.42	4.60	2,595
	1/2	550	3.64	5.61	2,595
20,000	Engine only	225	-------	3.35	
	1/6	400	.79	4.39	2,630
	1/4	531	1.77	4.92	
	1/2	531	2.65	5.74	
30,000	1/6	430	.56	4.48	
	1/4	508	1.24	5.26	2,630
	1/2	508	1.86	6.18	
40,000	1/6	492	.41	4.35	
	1/4	492	.81	5.43	2,630
	1/2	492	1.22	6.44	
50,000	1/6	492	.50	5.46	2,630
	1/2	492	.76	6.27	